

Small-Angle Neutron Scattering Studies on Amorphous Polystyrene Oriented by Solid-State Coextrusion

Georges Hadziioannou, Li-Hui Wang, Richard S. Stein,* and Roger S. Porter

Polymer Research Institute and Materials Research Laboratory, University of Massachusetts, Amherst, Massachusetts 01003. Received November 2, 1981

ABSTRACT: Small-angle neutron scattering measurements have been carried out on coextrusion oriented polystyrene to which deuterium-labeled polymer has been added. Radii of gyration of the deuterated component were determined in directions parallel and perpendicular to the extrusion direction. It was found for this sample, having a reasonably high molecular weight ($M_w = 6 \times 10^5$), that the anisotropy of radii of gyration agrees quantitatively with that predicted on the basis of an affine model, up to draw ratios of 10. This observation, in connection with parallel observations of sample contraction and of birefringence, suggests that for samples with molecular weights greater than the entanglement molecular weight, which are oriented in this manner, the molecular extension parallels the macroscopic sample extension.

1. Introduction

It is well-known that relaxed amorphous-state polymer chains exhibit a random "Gaussian" conformation.¹ It is therefore of interest to know how polymer conformation changes with external constraint. Small-angle neutron scattering (SANS) allows study of chain conformation directly in the solid state from the level of the whole macromolecule down to the statistical segment.

Previous theoretical studies^{2,3} on the scattering law for deformed polymer chains show the possibilities of describing the conformation by a general distribution function and of measuring the mean orientation of the statistical segment with respect to the stretching direction.² This latter information gives us the first moment of the orientation function and is thus complementary to that obtained by other methods such as birefringence and infrared dichroism, which give the second moment, or NMR anisotropy, with which one can obtain second, fourth, and higher moments.⁴

Conformational studies, by measuring the radius of gyration as well as orientation, aid in the understanding of how chains deform when stretched by different techniques and conditions. Indeed our purpose in this preliminary work is to study, mainly by SANS, the deformation mechanism of the chains on the oriented atactic amorphous polystyrene (PS) coextruded to high draw ratio within a billet of high-density polyethylene (HDPE).

Solid-state coextrusion is a unique method developed in this laboratory for producing polymers of high orientation and chain extension.⁵ By this technique cylindrical billets of HDPE are split longitudinally and extruded through a conical die after a film strip of the same or different thermoplastic has been inserted within the split. After extrusion, oriented films of the polymer inserted within the split are obtained simultaneously with the surrounding substrates. This method has been applied to semicrystalline polymers such as polyethylene, nylon 6, poly(vinylidene fluoride), and, recently, to atactic amorphous PS.^{6,7}

2. Experimental Section

2.1. Materials and Extrusion. The samples that we used were mixtures of 95% protonated and 5% completely deuterated atactic PS. The characteristics are $M_w = 6.0 \times 10^5$, $M_w/M_n < 1.10$ for the hydrogenated PS and $M_w = 5.4 \times 10^5$, $M_w/M_n < 1.12$ for the deuterated PS. The mixtures were prepared by dissolution in benzene at low concentration (<2%) followed by freeze-drying. Films of about 0.6-mm thickness were obtained by molding the PS powder blend under vacuum at 140 °C. Cylindrical billets of high-density polyethylene (Ultra Ethylux, Westlake Plastics), $3/8$ -in. diameter, were split longitudinally and a film strip $3/8$ in. wide of the PS mixture was inserted within the split prior to

extrusion. Thus oriented films of atactic polystyrene have been prepared under the compressive and extensional forces of the surrounding coextruded polyethylene substrates. The coextrusion was performed through a conical brass die in an Instron rheometer at a pressure of 280 kg/cm², a temperature of 127 °C, and a deformation rate of 0.1–0.2 cm/min to achieve an effective draw ratio ($EDR = L/L_0$, where L_0 and L are the lengths of the sample before and after extrusion, respectively) over a range of 1–10.

2.2. Small-Angle Neutron Scattering. The small-angle neutron scattering experiments were carried out at the National Center for Small Angle Scattering Research (NCSASR) located at the Oak Ridge National Laboratory (ORNL). The 30-m SANS facility was used with a pinhole collimation, a wavelength of 4.75 Å, and a two-dimensional multicounter (64 × 64 cells) placed 15 m from the sample. Each experiment was carried out in two successive scattering measurements, one for the background with the fully hydrogenated PS and a second with the PS solid solution of the hydrogenated and deuterated polymer mixture. The coherent signal which is related to the single-chain form factor for the deformed labeled chains was obtained by subtracting the background signal from the sample signal. The detector efficiency was calibrated with pure water, whose scattering is incoherent and thus essentially independent of angle.

2.3. Thermal Analysis. Thermal shrinkage experiments were performed on drawn PS samples by floating 10-mm-long strips in a glycerol bath. After reaching their equilibrium length, the films were cooled to room temperature and the dimensions redetermined. Shrinkage is defined as $S = (L_e - L_s)/L_e$ and the elastic recovery as $R = (L_e - L_s)/(L_e - L_0)$, where L_e is the length of the sample after extrusion, L_s is the length of the sample after shrinkage, and L_0 is the length of the original sample. The molecular draw ratio is defined as $MDR = (L_e - L_s + L_0)/L_0$.

2.4. Birefringence. Total birefringence was measured with a Zeiss polarizing microscope equipped with a calspar compensator. The thickness of the sliced samples was taken as the average of several micrometer measurements along the drawn films.

3. Results and Discussion

The SANS experiments were conducted in such a way that the scattered intensity is measured for all orientations of the scattering vector \mathbf{q} in the plane of the sample [$|\mathbf{q}| = q = (4\pi/\lambda) \sin(\theta/2)$, where λ is the wavelength of the neutron and θ is the angle between the incident and the scattered beam].

Scattering intensity contour diagrams for an unoriented and an oriented sample with $EDR = 4.2$ are given in Figures 1 and 2. The high anisotropy obtained for the drawn sample is evident.

The intensity falloff in a direction parallel to the extrusion direction occurs at too small a q value to allow a direct measurement of the component of the radius of gyration in the drawing direction, $(R_g)_\parallel$. In this direction, the scattering at small q is obscured by the beam stop. The radius of gyration in the transversal direction, $(R_g)_\perp$, is obtained by using the Zimm plot type analysis restricted

Table I
Values of Radius of Gyration in the Transversal and Longitudinal Directions, the Total Birefringence, Orientation Function, and Number of Statistical Segments between Entanglements vs. EDR

draw ratios for PS			radius of gyration				$-\Delta n \times 10^3$	f^a	n^b
EDR from marking	MDR from SANS	MDR from shrinkage	$(R_g)_\perp^{\text{exptl}}$, Å	$(R_g)_\perp^{\text{aff}}$, Å	$(R_g)_\parallel^{\text{calcd}}$, Å	$(R_g)_\parallel^{\text{aff}}$, Å			
1.0	1.0	1.0	202	202	202	202			
2.9	2.8	2.9	134	118	630	590	6.0	0.05	32
4.2	4.1	4.0	102	99	850	850	16.7	0.14	25
5.1	5.0	5.0	95	90	1060	1030	19.4	0.16	32
9.6	8.6	9.4	62	65	1645	1940	32.6	0.27	68

^a From birefringence measurements. ^b Number of statistical segments between entanglements.

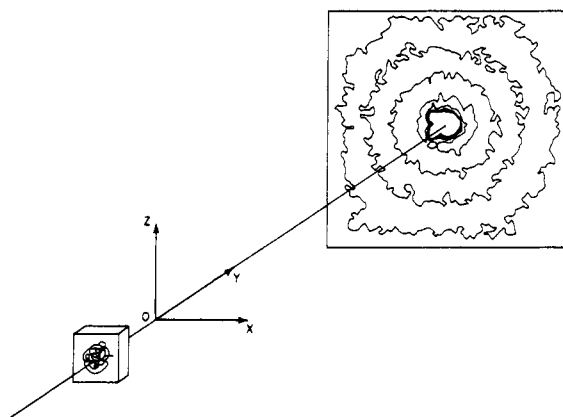


Figure 1. Geometry of SANS experiment and intensity contour plot for scattering from the unoriented amorphous polystyrene. The difference between the normalized intensity of the outer and the inner contour levels is about 200.

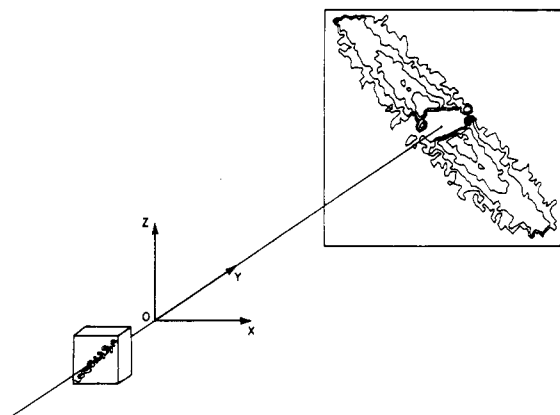


Figure 2. Geometry of SANS experiment and intensity contour plot for scattering from the oriented amorphous polystyrene, EDR = 4.2. The difference between the normalized intensity of the outer and the inner contour levels is about 100.

into the Guinier region ($qR_g < 1$). These values are reported in Table I and plotted in Figure 3.

The scattering laws in the Guinier region, based on the affine transformation of the radius of gyration and constant volume, should be

$$S_\perp(q) = 1 - \frac{q_\perp^2 (R_g^2)_\perp}{3} = 1 - \frac{q_\perp^2 (R_g^2)_0}{3(\text{MDR})} \quad (1)$$

$$S_\parallel(q) = 1 - \frac{q_\parallel^2 (R_g^2)_\parallel}{3} = 1 - \frac{q_\parallel^2 (\text{MDR})^2 (R_g^2)_0}{3} \quad (2)$$

Considering the equal-intensity contours in the anisotropic patterns and relations 1 and 2, we are able to calculate from the ratio of q_\perp/q_\parallel [$q_\perp/q_\parallel = (R_g)_\parallel/(R_g)_\perp = (\text{MDR})^{3/2}$] indirectly the molecular draw ratio (MDR) and

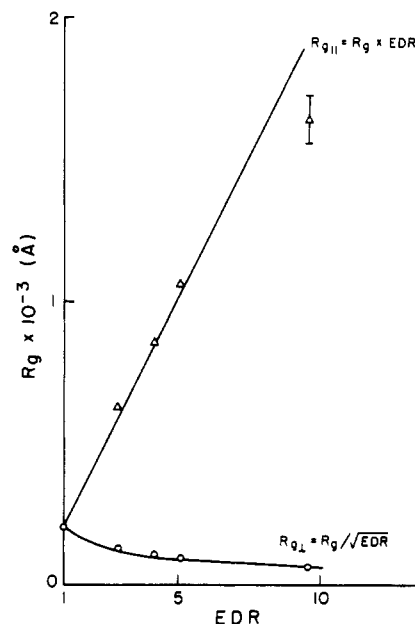


Figure 3. Radius of gyration as a function of EDR: (O) transversal radius of gyration, $(R_g)_\perp$; (Δ) longitudinal radius of gyration, $(R_g)_\parallel$. The continuous lines represent the variations of the radius of gyration assuming an affine transformation and constant volume.

the radius of gyration in a direction parallel to the extrusion $(R_g)_\parallel$. Even though the equal-intensity contour lines at small q are obscured by the beam stop in the $(R_g)_\parallel$ direction, it is possible to interpolate them into this region from data at other azimuthal angles not obscured by the beam stop, as can be seen from inspection of Figure 2. The MDR values calculated from the ratio q_\perp/q_\parallel and those from the shrinkage experiments are reported in Table I.

In Figure 3 we have also plotted the calculated values for the radius of gyration in the longitudinal direction [$(R_g)_\parallel$]. The continuous lines on this plot represent the variation of the coil dimensions in the transversal and the longitudinal directions, assuming an affine transformation and constant volume. Our experimental values of the radius of gyration and those predicted by the affine transformation law are in very good accord.

The agreement between the MDR and EDR is also excellent, indicating that under the drawing conditions we used, the radii of gyration deform effectively in the same manner as the external dimensions and the drawing efficiency is nearly perfect.

The efficiency of drawing was measured also by the thermal shrinkage method described above. The drawn amorphous specimens retract to near their original shape upon rapid heating to a temperature sufficiently above T_g . The high efficiency of drawing is reflected in Figure 4, where the shrinkage recovery is plotted as a function of

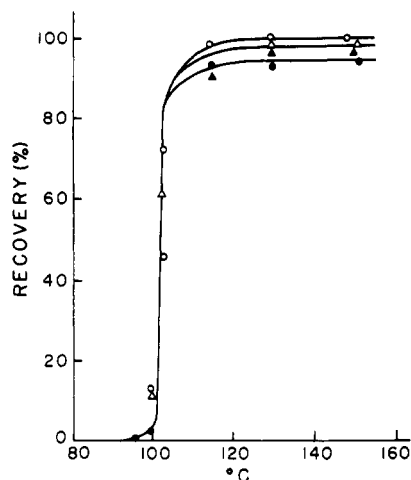


Figure 4. Elastic recovery as a function of shrinkage temperature for samples of different draw ratios: (O) EDR = 4.2, hydrogenated polystyrene; (Δ) EDR = 9.0, hydrogenated polystyrene; (●) EDR = 4.2, deuterated/hydrogenated polystyrene; (▲) EDR = 9.6, deuterated/hydrogenated polystyrene.

temperature. Almost a total recovery is observed for temperatures $\sim 160^\circ\text{C}$!

The molecular draw ratio calculated from thermal shrinkage also expresses the efficiency of draw. The values reported in Table I show good agreement with those measured by SANS and EDR. The fact that the MDR's from shrinkage and SANS agree also confirms that the technique of measuring MDR by thermal shrinkage can be valid.

The glass transition (T_g) is independent of draw as measured by elastic recovery on warming (see Figure 4). This result is consistent with the constancy of the volume vs. EDR.⁹

Birefringence measurements give an indication of orientation in those extended molecules. As expected, efficiently drawn samples exhibit pronounced birefringence (Figure 5 and Table I), with systematic increases with draw ratio. The segmental orientation is also quantified by the Hermans orientation function f (see Table I) computed from the birefringence measurements (see relation 56, ref 8) [the mean value of α is 38° measured by IR with the 2850-cm^{-1} band]. The orientation function, f , is also related to the number of statistical segments between the entanglements, n , in a rubberlike polymer by the relation $f = (1/5n)[(\text{EDR})^2 - 1/(\text{EDR})]$.¹⁰ We calculated this number n (see Table I) and found that for up to 5 times extension of the chains we have a constant number of statistical segments between entanglements and after that for 10 times extension this number is double. The number of monomer units per statistical segment can also be evaluated by assuming that the molecular weight between entanglements is equal to 35 000.¹¹ In fact, we found that this number is approximately equal to 10, which is in good concordance with the values reported in the literature.¹¹ This also means that entanglements effectively hold to near maximum network draw of near 5 followed by disentanglement at yet higher draw.

4. Conclusion

Results in this preliminary work are consistent with the model of chain entanglements, at least for the molecular

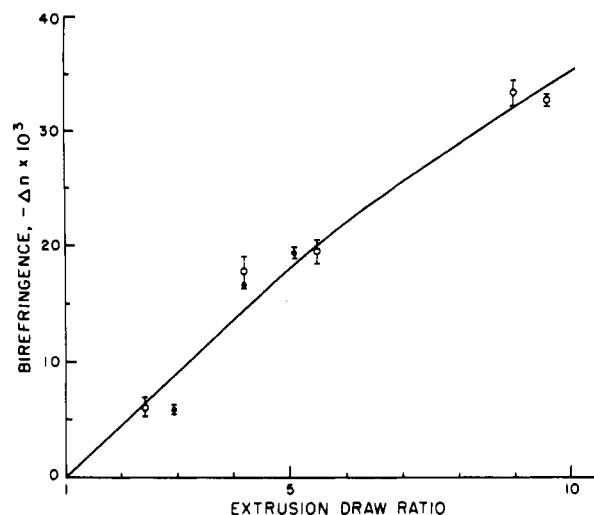


Figure 5. Birefringence of drawn polystyrene as a function of EDR.

weight of the PS studied. The entanglements restrict the molecules from slipping past each other on the solid-state extrusion, therefore facilitating chain extension and concomitant orientation. These two former processes were also aided by the low deformation temperature. Furthermore, this chain extension takes place in the same manner as in the macroscopic scale, following the same laws of the affine deformation.

The efficiency of draw is shown to be nearly perfect (affine), with concordant results up to a molecular draw ratio for PS at least 10 times as measured by SANS, elastic shrinkage after draw, and marker displacement during draw (EDR).

Recent experiments with lower molecular weight PS have shown that the draw efficiency is less perfect, as indicated by measurements of thermal shrinkage and SANS. This latter result will be reported in a following paper together with large q range SANS measurements.

Acknowledgment. We are thankful to NSF for financial support and to the staff of NCSASR (ORNL) for assistance, in particular, G. D. Wignall.

References and Notes

- (1) Cotton, J. P.; Decker, D.; Benoit, H.; Farnoux, B.; Picot, C.; Jannink, G.; Ober, R.; des Cloizeaux, J. *Macromolecules* **1974**, *7*, 863.
- (2) Benoit, H.; Duplessix, R.; Ober, R.; Daoud, M.; Cotton, J. P.; Farnoux, B.; Jannink, G. *Macromolecules* **1975**, *8*, 451.
- (3) Pearson, D. S. *Macromolecules* **1977**, *10*, 696.
- (4) Ward, I. M. "Mechanical Properties of Solid Polymers"; Wiley-Interscience: New York, 1971.
- (5) Griswold, P. D.; Zachariades, A. E.; Porter, R. S. In "Flow-Induced Crystallization in Polymer Systems"; Miller, R. L., Ed.; Gordon and Breach: New York, 1979; pp 205-211.
- (6) Zachariades, A. E.; Sherman, E. S.; Porter, R. S. *J. Appl. Polym. Sci.* **1979**, *24*, 2137.
- (7) Zachariades, A. E.; Sherman, E. S.; Porter, R. S. *J. Polym. Sci., Polym. Lett. Ed.* **1979**, *17*, 255.
- (8) Stein, R. S. *J. Appl. Phys.* **1961**, *32*, 1280.
- (9) Appelt, B.; Wang, L. H.; Porter, R. S. *J. Mater. Sci.* **1981**, *16*, 1763.
- (10) Kuhn, W.; Grun, F. *Kolloid-Z.* **1942**, *101*, 248.
- (11) Jenkins, R.; Porter, R. S. *Adv. Polym. Sci.* **1980**, *36*, 1.